Thermodynamic Characterization of the Interaction between CAR−RXR and SRC-1 Peptide by Isothermal Titration Calorimetry†

Edward Wright, Jeremy Vincent, and Elias J. Fernandez*

Department of Biochemistry and Cellular and Molecular Biology, University of Tennessee, Knoxville, Tennessee 37996

Received August 10, 2006; Revised Manuscript Received November 13, 2006

ABSTRACT: The constitutive androstane receptor (CAR) enhances transcription of specific target genes that regulate several metabolic pathways. CAR functions as an obligate heterodimer (CAR−RXR) with the retinoid X receptor (RXR). Also part of the active receptor complex is the steroid receptor coactivator-1 (SRC-1) which interacts with the receptor complex via specific receptor interaction domains (RIDs). A peptide derived from SRC-1 RID2 is used to study the thermodynamic properties of the interaction with the CAR−RXR ligand binding domain (LBD) complex. In the absence of ligands for both CAR and RXR, binding of coactivator peptide to the CAR−RXR heterodimer is characterized by a favorable enthalpy change and an unfavorable entropy change. The addition of the CAR agonist, TCPOBOP, increases the affinity for coactivator by decreasing the unfavorable entropy and increasing the favorable intrinsic enthalpy of the interaction. The RXR ligand, 9-*cis*-RA, generates a second SRC-1 site and increases the affinity by improving the entropic component of binding. There is an additional increase in affinity for one of the two sites in the presence of both ligands. The change in heat capacity (ΔC_p) is also investigated. A 2-fold difference in ΔC_p is observed between liganded and unliganded CAR−RXR. The observed thermodynamic parameters for binding of SRC-1 peptide to liganded and apo CAR−RXR as well as the difference in the ΔC_p data provide evidence that the apo CAR−RXR heterodimer is conformationally mobile. The more favorable enthalpic contribution for TCPOBOP-bound CAR−RXR indicates that preformation of the binding site improves the complementarity of the coactivator−receptor interaction.

Activated nuclear receptors (NRs)[1] recruit p160 transcriptional coactivators such as SRC-1/NCoA-1 and TIF2/GRIP/NCoA-2 and other coactivator proteins (Figure 1A) (*1*). These p160 coactivators, in turn, can interact with CBP/p300 and associated molecules with histone acetyltransferase activity and activate the basal transcription machinery of the cell (*2*). When the NR binds agonist ligand, there is a conformational change in the C-terminus that results in a hydrophobic docking site for coactivator proteins such as SRC-1 (*3*). There are four unique receptor interaction domains (RIDs) in SRC-1 that can interact with the NR (*4*). Each RID contains a core amino acid motif that includes the sequence LXXLL (X being any amino acid). Since an NR can bind only a single RID at once, specificity of NRs for a particular RID on SRC-1 is determined by the amino acids that flank this LXXLL motif (*5*). Short peptides of up to 13 amino acids based on the sequence of the RID have been observed to bind NRs through specific apolar, hydrogen bond, and salt bridge interactions in X-ray crystal structures (*3*, *6*−*9*). In these structures, the conformation of these peptides is always helical, although the conformation of the RID within the free SRC-1 molecule is unknown.

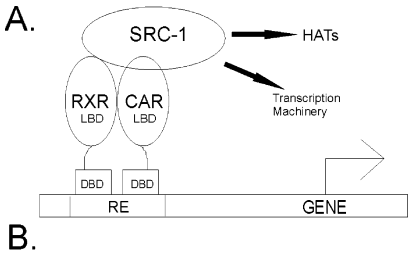

FIGURE 1: (A) Nuclear receptors are modular proteins containing an N-terminal DNA binding domain (DBD) which binds specific response elements (REs) upstream of the target gene and a C-terminal ligand binding domain (LBD) which binds small molecule ligands and recruits coactivator proteins such as SRC-1. The coactivator protein interacts with proteins which possess histone acetyltransferase activity (HATs) as well as the basal transcriptional machinery for enhancing transcription of the target gene. (B) Sequence of the 13-residue peptide from SRC-1 used in the binding studies. The LXXLL motif is underlined.

NR proteins share a conserved domain architecture. X-ray structures of the ligand binding domains (LBDs) of all NRs determined to date exhibit a common three-dimensional fold. The LBD which is situated in the C-terminus of the NR encloses the ligand binding pocket within a 12-α-helix

† This research was supported by Grant R01-DK 066394 from the National Institutes of Health.

* To whom correspondence should be addressed: Department of Biochemistry, Cellular and Molecular Biology, University of Tennessee, Knoxville, TN 37996-0840. Telephone: (865) 974-4090. Fax: (865) 974-6306. E-mail: elias.fernandez@utk.edu.

[1] Abbreviations: CAR, constitutive androstane receptor; RXR, retinoid X receptor; SRC-1, steroid receptor coactivator-1; RID, receptor interaction domain; LBD, ligand binding domain; TCPOBOP, 1,4-bis-[2-(3,5-dichloropyridyloxy)]benzene; 9-*cis*-RA, 9-*cis*-retinoic acid; NR, nuclear receptor; ITC, isothermal titration calorimetry; AF2, activation function 2; TCEP, tris(2-carboxyethyl)phosphine.

10.1021/bi061627i CCC: $37.00
Published on Web 12/21/2006

framework. When the agonist binds, the C-terminal helix (H12) undergoes the largest conformational change, thereby activating the ligand-dependent activation function 2 (AF2) domain. In the agonist-bound active conformation, H12 is packed against the body of the LBD. In this position, H12 and residues from helix H3 create the hydrophobic cleft that interacts with the coactivator RID (*10*).

The constitutive androstane receptor (CAR) belongs to the NR superfamily and plays key roles in the clearance of both xenobiotics (*11*, *12*) and endogenous toxins such as bilirubin (*13*). CAR is largely expressed in the liver and intestine where it controls the transcription of specific genes, including P450 monooxygenases, phase II conjugating enzymes, and xenobiotic transporters. This activity of CAR can also be deleterious as CAR-mediated metabolism of acetaminophen results in a toxic reactive quinone metabolite (*N*-acetyl-*p*-benzoquinone). While classical NRs are inactive in the absence of ligand, CAR displays strong ligand-independent activity which implies that the H12/AF2 conformation in apo CAR is in the active-state conformation. As with many NRs, CAR functions as a heterodimeric partner of the retinoid X receptor-α (RXRα) and in the active state can recruit the coactivator protein SRC-1 by interacting specifically with RID2 of SRC-1 (*14*). CAR activity can be reversed by inverse agonists such as androstenol (5α-androst-16-en-3α-ol) (*15*). Although constitutively active, CAR activity can be enhanced by agonist ligands such as 1,4-bis[2-(3,5-dichloropyridyloxy)]benzene (TCPOBOP) (*16*) and 6-(4-chlorophenyl)imidazol[2,1-*b*][1,3]thiazole-5-carbaldehyde *O*-(3,4-dichlorobenzyl)oxime (CITGO) (*17*) that are selective for murine and human CAR, respectively. CAR−RXR heterodimer (CAR−RXR) activity is also increased by the binding of RXR agonists such as 9-*cis* retinoic acid to RXR (*18*).

Crystal structures of CAR LBDs reveal that binding of ligand alters the conformation of helix 12 (AF2). The inverse agonist, androstenol, disrupts the interactions of H12/AF2 with the LBD, while the agonists TCPOBOP and CITGO stabilize the active-state conformation of H12/AF2 so that coactivator binding is favored, in mCAR and hCAR, respectively (*7*, *19*, *20*). Although mutagenesis has shown that the same structural elements are required for ligand-independent recruitment of coactivator proteins by CAR (*14*), less is known about the differences between coactivator binding to apo versus agonist-bound CAR−RXR heterodimer. Because CAR can recruit coactivator without bound agonist, this nuclear receptor provides the rare opportunity to compare binding of coactivator proteins in the presence and absence of ligands. Here, we describe the thermodynamics of binding of a thirteen residue peptide based on RID2 of SRC-1 to the CAR−RXR heterodimer using isothermal titration calorimetry (ITC) (Figure 1B). RID2 has been shown to be critical for binding fo SRC-1 to CAR and also binds RXR in the presence of RXR agonist (*14*, *21*). ITC has been commonly used to analyze protein−peptide (*22*−*24*), protein−protein (*25*−*27*), and protein−ligand or −substrate interactions (*28*). Previously, thermodynamic properties of binding of the coactivator to the androgen receptor have been determined using peptides derived from coactivator protein (*29*). In this study, the mCAR−hRXR LBD heterodimer is used as the model system to characterize the thermodynamics of NR−coactivator interactions. Our data provide a detailed thermodynamic profile of the interactions of CAR−RXR with SRC-1 peptide, including the changes in free energy, enthalpy, entropy, and heat capacity. We have determined that the improved binding of SRC-1 peptide to agonist-bound CAR in the heterodimer has both enthalpic and entropic components. We also show that the thermodynamic basis for agonist-mediated enhancement of coactivator recruitment is different in the CAR monomer and CAR−RXR. Evidence of allosteric communication between LBDs when both ligands are present is provided. Finally, heat capacity changes and structural energetics are used to demonstrate that apo CAR−RXR is more conformationally mobile than CAR(TCPOBOP)−RXR.

EXPERIMENTAL PROCEDURES

Reagents. Purified SRC-1 peptide (^{687}ERHKILHRLLQEG^{699}) was purchased from the W. M. Keck Biotechnology Resource Center at Yale University (New Haven, CT). TCPOBOP was purchased from Calbiochem, and 9-*cis*-RA was purchased from MP Biomedicals.

Protein Expression and Purification. The murine CAR LBD (residues 117−358) was subcloned into pET15b with an N-terminal hexahistidine tag from mCAR cDNA kindly provided by B. M. Forman. The human RXRα LBD (residues 225−462) was subcloned into the pACYC184 vector and was a kind gift from B. Wisely (Glaxo SmithKline, Inc.). The two plasmids were cotransformed into *Escherichia coli* BL21(DE3) Gold cells (Novagen). After being induced with 0.5 mM IPTG, the cells were grown for 18−22 h at 20 °C and harvested by centrifugation. The cells were lysed with a French press (two passes at 20 000 psi). The CAR−RXR heterodimer was first purified from the cleared lysate using Ni-NTA affinity (Qiagen) and subsequently by size-exclusion chromatography using Superdex 75 resin (GE Healthsciences). The concentration of the protein was quantified using the Bio-Rad protein assay kit with bovine serum albumin as the standard. For use in ITC experiments, a more stable form of the CAR LBD was obtained by mutating a surface cysteine, distal from the SRC-1 binding site, to a serine residue. From cell-based transcription assays, this mutant form of CAR appears to have a transcriptional profile identical to that of wild-type CAR (data not shown). Henceforth, the CAR protein used in the assays below is the C221S mCAR LBD.

Isothermal Titration Calorimetry. ITC experiments were performed using a VP_ITC microcalorimeter from Microcal, Inc. Purified CAR−RXR complex was dialyzed extensively against the buffer used in the ITC experiments. The following buffers were used: 50 mM HEPES, 0.1 M NaCl, and 1 mM TCEP; and 50 mM Tris-HCl, 75 mM NaCl, 1 mM TCEP, 50 mM Phosphate, and 1 mM TCEP. The variation in NaCl concentration maintained a constant ionic strength for comparison of binding in different buffers. Stock ligand solutions were prepared in dimethyl sulfoxide (DMSO). Ligand concentrations were in 5-fold molar excess of CAR−RXR, which is at least 10 times the ligand−receptor dissociation constant in all titrations. Equivalent amounts of ligand were added to both protein and peptide solutions, and the DMSO concentration was adjusted to 3.5% for all titrations, including those in the absence of ligand. Titrations consisted of 29 injections of 10 μL and were separated by

240 s. Each titration contained 2−40 μM CAR−RXR in the sample cell. Concentrations of SRC-1 peptide in the injection syringe ranged from 90 to 550 μM. For titrations using the CAR monomer, the sample cell contained 25−40 μM protein and the injection syringe contained from 0.40 to 1.0 mM SRC-1 peptide. For all titrations, the c values [$c = K_a M_t$, where M_t is the concentration of macromolecule binding sites (*30*)] ranged from 8 to 32. These values are within the ideal range for determining binding constants by ITC. In early experiments, gel filtration was performed to verify that the quaternary state of the protein had not been altered during the titration (Figure S1 of the Supporting Information).

All data were fit using Origin 5.0 (Microcal, Inc.) to determine the binding constant (K_a), apparent stoichiometry (N), and changes in binding free energy (ΔG), enthalpy (ΔH), and entropy (ΔS) (*30*).

The extent of binding-linked protonation is calculated using the equation

$$\Delta H_{obs} = \Delta H_{int} + N_H \Delta H_{ion} \quad (1)$$

where ΔH_{obs} is the observed enthalpy change, ΔH_{int} is the intrinsic enthalpy change, N_H is the net number of protons taken up during the binding process, and ΔH_{ion} is the ionization enthalpy of the buffer from ref *31*. Extrapolation of ΔH_{obs} to a value of zero buffer ionization (y-intercept) gives ΔH_{int}.

The change in heat capacity is determined using the equation

$$\Delta C_p = \frac{\delta \Delta H_{int}}{\delta T} \quad (2)$$

The ionization enthalpies for the individual buffers at each temperature were obtained from previous studies (*31*, *32*). The extent of proton transfer and ΔH_{int} was determined at each temperature using eq 3, and the resulting ΔH_{int} values were plotted as a function of temperature to find ΔC_p.

Solvent Accessible Surface Area Calculation and Theoretical ΔC_p. The *access_surf* program within the NMR_Refine module of Insight II (Accelrys) was used to calculate solvent accessible surface area (1.4 Å solvent radius) from the structure of the CAR−RXR heterodimer with TCPOBOP, 9-*cis*-RA, and coactivator peptides bound (PDB entry 1XLS). Surface areas were calculated for each atom and added to obtain the total polar and apolar solvent-exposed surface areas. First, the solvent accessible surface area was computed for the entire complex of liganded protein and bound coactivator peptides. Next, the solvent accessible surface area for the coactivator-free protein complex was computed by simply omitting the coordinates of the coactivator peptide from the structure. Finally, the solvent accessible surface area of the free peptide was determined by omitting the coordinates of CAR(TCPOBOP)−RXR(9-*cis*-RA). The change in polar and apolar solvent accessible surface area was determined by subtracting the values obtained from free heterodimer and free peptide from the values obtained from the heterodimer−peptide complex. For computation of the theoretical value of ΔC_p from the structure, the equations developed by Murphy and Freire (*33*)

$$\Delta C_p = 0.54 \Delta ASA_{apolar} - 0.26 \Delta ASA_{polar} \quad (3)$$

and Spolar et al. (*34*)

$$\Delta C_p = 0.32 \Delta ASA_{apolar} - 0.14 \Delta ASA_{polar} \quad (4)$$

were used.

In the equations given above, ΔASA is the change in either apolar or polar solvent accessible surface area in square angstroms and ΔC_p is the change in heat capacity in calories per kelvin per mole.

RESULTS AND DISCUSSION

In this study, ITC was used to characterize the binding of the coactivator to the LBDs of various CAR−RXR complexes, including apo CAR−RXR, CAR(TCPOBOP)−RXR, CAR−RXR(9-*cis*-RA), CAR(TCPOBOP)−RXR(9-*cis*-RA), monomeric CAR and CAR(TCPOBOP). Titrations in the presence of the inverse agonist, androstenol, could not be performed because of precipitation in the sample cell even at low ligand concentrations. Since the SRC-1 peptide binds both CAR and RXR, a total of two possible binding sites for this peptide are present on the CAR−RXR heterodimer. Peptides similar in length have been cocrystallized with other NRs (*7*, *9*), and the peptide used in this study has been cocrystallized with the human CAR−RXR heterodimer (*20*). Amino acids flanking the 13-residue core do not appear to play a significant role in CAR−RXR binding since a SRC-1 RID2-based 21-amino acid peptide containing this 13-residue core exhibits no difference in affinity or enthalpy from the 13-amino acid peptide (data not shown). Representative titrations for the 13-amino acid residue peptide binding to CAR−RXR complexes are shown in Figures 2 and 3. The data are summarized in Tables 1 and 2.

Binding-Linked Protonation. The observed enthalpy change due to binding contains contributions from the protonation or deprotonation of the buffering system (*35*, *36*). In this study, binding of the SRC-1 peptide to CAR−RXR can result in a pK_a shift for a residue on the peptide or macromolecule. To accommodate this change in pK_a, protons are either taken up from or released to the buffer. To determine the extent of this phenomenon in the interaction between SRC-1 peptide and CAR−RXR heterodimer, the titrations were performed in three separate buffers, each with a different heat of ionization. The observed enthalpy was plotted versus the heat of ionization of each buffer and the net uptake of protons determined from the slope (Figure 4). The net uptake is close to zero in the presence of either TCPOBOP (0.079) or 9-*cis*-RA (0.033). In contrast, there is a small net release of protons when the SRC-1 peptide is titrated into apo CAR−RXR (−0.18) (Table 3). This net release is due to changes in the pK_a of one or more ionizable groups on either SRC-1 peptide or CAR. Since the net uptake is different for apo versus liganded CAR, the contribution from buffer ionization to total enthalpy must be considered when one is comparing binding to the different CAR−RXR complexes.

Comparison of Energetics of Binding of SRC-1 to Apo and Holo CAR in the CAR−RXR Heterodimer. There is evidence that the CAR−RXR heterodimer can recruit SRC-1, leading to transcription of genes, in the absence of agonist (*37*). In the absence of an apo CAR:SRC-1−RXR complex structure, we have used ITC to characterize the recruitment of the SRC-1 13-amino acid peptide by the LBDs of apo CAR−RXR. As expected, the data for titrations of SRC-1 peptide

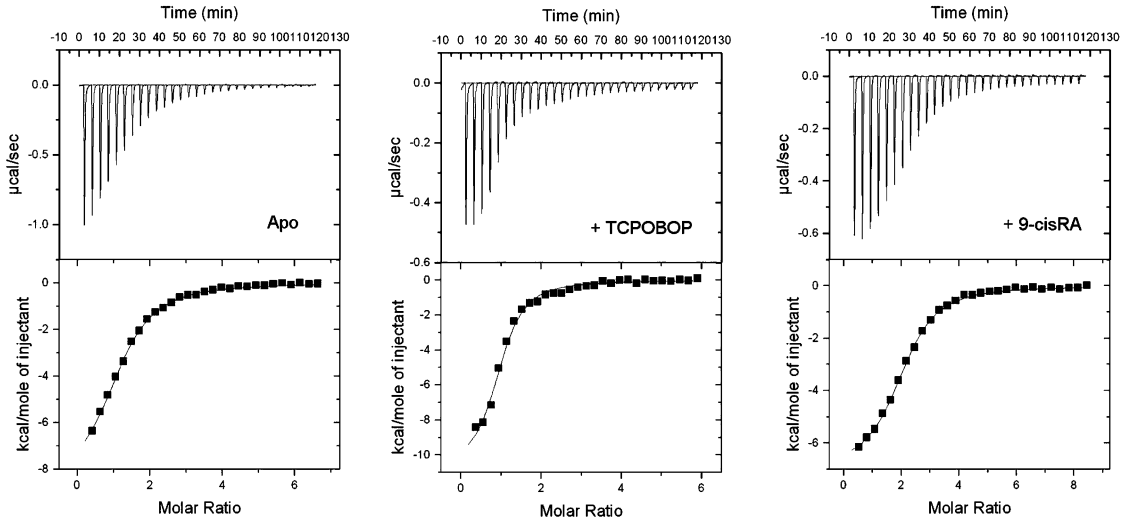

FIGURE 2: Representative titrations of SRC-1 peptide into CAR−RXR in the absence of ligand (left), in the presence of TCPOBOP (middle), and in the presence of 9-*cis*-RA (right). Titrations contained 50 mM phosphate buffer and 1 mM TCEP at pH 7.2.

into the apo heterodimer fit well to the one-site binding model and the apparent stoichiometry for the interaction is one peptide molecule per CAR−RXR heterodimer (Figure 2). The affinity (K_d) ranges from 4.9 to 6.3 μM, depending on the buffer system that was used (Table 1). Furthermore, we note that the binding is enthalpically favorable (negative ΔH) but entropically unfavorable (negative $T\Delta S$). The measured enthalpy values of −9.2, −10.0, and −11.1 kcal/mol most likely reflect the contributions from the four charged residues on CAR which directly interact with the coactivator (*7*). Lysine 187 of helix H3 and glutamate 355 of helix H12/AF2 in mCAR bind to residues at either end of the short, α-helical, coactivator peptide. These "charge clamp" interactions are a common feature in NR−coactivator complexes (*3*). In the crystal structure, the E355 side chain forms a hydrogen bond with the backbone amide of the leucine immediately preceding the LXXLL motif (position −1) in TIF2 (*7*). In SRC-1, this residue is an isoleucine. The K187 side chain H bonds with the backbone carbonyl of the leucine in the +5 position of the LXXLL motif (Figure S2A of the Supporting Information). This residue is conserved in both TIF2 and SRC-1. Additionally, E198 and K193 in CAR (helices H4 and H3′) form salt bridges with arginine (+2) and aspartic acid (+6) in TIF2, respectively (*7*). Positions +2 and +6 are histidine and glutamine in SRC-1, respectively, which can also H bond with E198 and R193 on CAR. ITC measures the global thermodynamic parameters of a system so the net ΔH is not merely the sum of these four hydrogen bonds, changes in protein−solvent and peptide−solvent interactions, and changes in bonding within the protein and peptide also contribute. Nevertheless, the formation of these four hydrogen bonds will contribute significantly to ΔH. Besides these H bonding interactions, the interface of the SRC-1 peptide and CAR is predominantly apolar. While the burial of such exposed hydrophobic faces is expected to result in favorable entropy (positive $T\Delta S$), the observed change in entropy in our titration appears to be unfavorable (−2.8 kcal/mol). The observed $T\Delta S$ can arise from two events, the burial of apolar surfaces (favorable $T\Delta S$) and a restriction of CAR mobility (unfavorable $T\Delta S$). Evidence that NRs exist in a continuum of conformationally mobile states and that the presence of ligand restricts this mobility is accumulating (*38*). The most significant changes upon ligand binding are observed in the conformation of helix H12/AF2 (*10*). Binding of SRC-1 peptide can also restrict CAR mobility, resulting in a decrease in entropy (unfavorable $T\Delta S$). Thus, the net loss in degrees of freedom in the CAR−SRC-1 complex is larger than the favorable $T\Delta S$ from burial of the apolar faces of CAR and the SRC-1 peptide.

Although CAR is constitutively active, its transcriptional activity can be enhanced by TCPOBOP approximately 3-fold with an EC_{50} of 0.1 μM (*39*). The role of the CAR agonist on SRC-1 recruitment was studied by performing the titration in the presence of saturating amounts of TCPOBOP. In this titration, the SRC-1 peptide is expected to interact only with CAR since RXR is in the unliganded inactive form. As anticipated, this data fit well with the single-site binding model with a stoichiometry of one SRC-1 peptide molecule per CAR(TCPOBOP)−RXR complex. There is an almost 10-fold increase in affinity ($K_d = 0.6$ μM) compared to that of apo CAR−RXR, a consequence of both favorable enthalpy and favorable entropy (Figure 2 and Table 1). The seemingly more favorable ΔH for apo versus liganded CAR−RXR results from contributions of buffer ionization. The intrinsic ΔH is most favorable for CAR(TCPOBOP)−RXR ($\Delta H_{int} = -10.2$ kcal/mol) compared to apo CAR−RXR (−9.1 kcal/mol) (Figure 4 and Table 3).

In all three buffers that were used, the presence of TCPOBOP results in a decrease in the entropic penalty for the formation of the CAR−SRC-1 peptide complex. From a thermodynamic perspective, the binding of TCPOBOP reduces the difference in entropy between free CAR−RXR and CAR:SRC-1−RXR. Thus, the increased levels of transcription upon binding of TCPOBOP may result predominantly from the stabilization of the CAR−RXR complex with an additional contribution from a more favorable enthalpy.

Effect of 9-cis-RA on Binding of SRC-1 to the Apo and TCPOBOP-Bound CAR−RXR Heterodimer. In the presence of 9-*cis*-RA, the RXR AF2 domain adopts the active NR conformation and can recruit coactivator proteins (*40*). NR−RXR heterodimers respond differently to concurrent activation of both the NR and RXR and can be grouped into three broad categories. A permissive NR−RXR heterodimeric

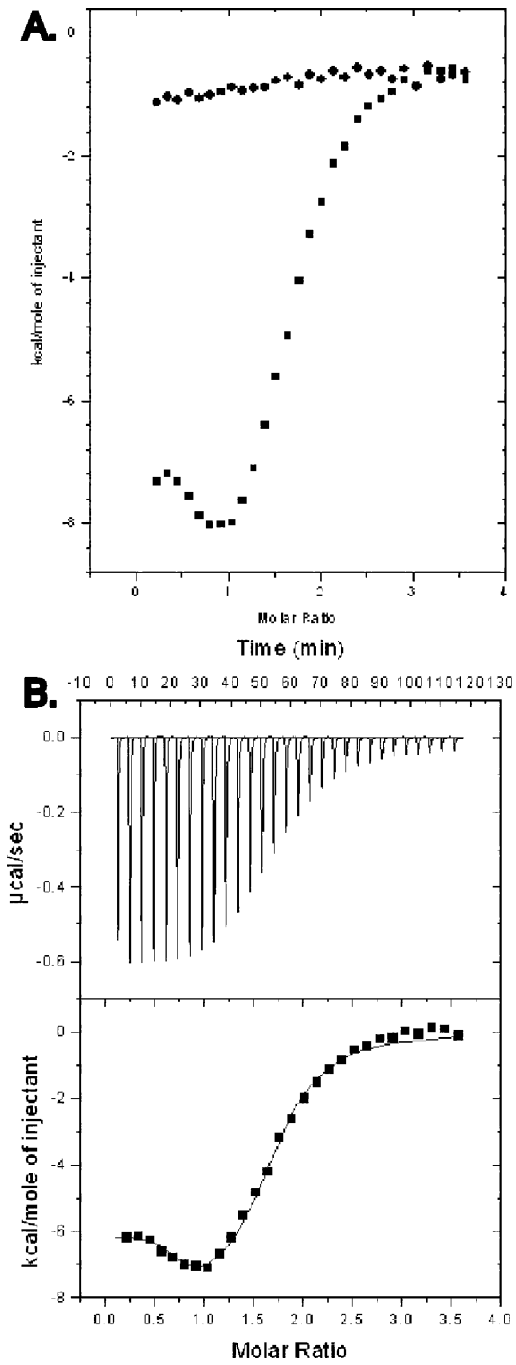

FIGURE 3: (A) Titration of SRC-1 peptide into CAR−RXR in the presence of both TCPOBOP and 9-*cis*-RA. Data points represent the integration of the raw data for the titrations. Titrations of peptide into buffer and ligands were performed to determine background. (B) Data points resulting from subtraction of background and subsequent curve fitting to the data.

complex can be activated by agonists for either the NR or RXR, and the agonist activity is additive with both agonists present. Conditional heterodimers are activated by either the NR agonist or both NR and RXR agonists but are unresponsive to RXR agonist alone. Nonpermissive heterodimer association occurs when the complex is activated by NR agonist alone (*41*). The CAR constitutive activity makes it difficult to be categorized in the groups listed above. The effect of 9-*cis*-RA on CAR activity in the absence of TCPOBOP depends on the nature of the response element on the target DNA. In ER-6-type response elements, RXR

Table 1: Thermodynamic Parameters for Binding of SRC-1 Peptide to CAR−RXR in the Presence of the Indicated Ligands[a]

ligand	K_d (μM)	ΔH (kcal/mol)	$-T\Delta S$ (kcal/mol)	ΔG (kcal/mol)	N[b]
		HEPES Buffer			
TCPOBOP	0.60 ± 0.1	−10.0 ± 0.3	1.5	−8.5	0.98 ± 0.07
9-*cis*-RA	1.5 ± 0.2	−7.9 ± 0.3	0.0	−7.9	2.04 ± 0.09
none	4.9 ± 0.7	−10.0 ± 0.4	2.8	−7.2	1.03 ± 0.06
		Phosphate Buffer			
TCPOBOP	0.62 ± 0.1	−10.1 ± 0.2	1.6	−8.5	1.01 ± 0.03
9-*cis*-RA	1.7 ± 0.1	−7.5 ± 0.1	0.4	−7.9	1.98 ± 0.05
none	6.3 ± 0.5	−9.2 ± 0.4	2.1	−7.1	1.04 ± 0.05
		Tris Buffer			
TCPOBOP	0.63 ± 0.1	−9.3 ± 0.2	1.2	−8.5	0.96 ± 0.09
9-*cis*-RA	2.1 ± 0.3	−8.1 ± 0.4	0.4	−7.7	2.03 ± 0.09
none	5.4 ± 0.5	−11.1 ± 0.2	3.9	−7.2	1.02 ± 0.05

[a] Determined at 25 °C and pH 7.2 as described in Experimental Procedures. The reported values are the average of three experiments, and the errors are the standard deviation. [b] The apparent stoichiometry from the curve fitting data.

Table 2: Thermodynamic Parameters for Binding of SRC-1 Peptide to CAR−RXR in the Presence of 9-*cis*-RA and TCPOBOP[a]

	K_d (μM)	ΔH (kcal/mol)	$-T\Delta S$ (kcal/mol)	ΔG (kcal/mol)	N[b]
site one	0.10 ± 0.04	−5.9 ± 0.4	−3.7	−9.6	0.93 ± 0.06
site two	1.2 ± 0.2	−9.2 ± 0.5	1.0	−8.2	1.04 ± 0.08

[a] Determined at 25 °C and pH 7.2 in 50 mM HEPES, 0.1 M NaCl, and 1 mM TCEP. The reported values are the average of five experiments, and the errors are the standard deviation. [b] The apparent stoichiometry from the curve fitting data.

agonist alone has been shown to enhance transcription via CAR(apo)−RXR (*18*). To determine the effect of 9-*cis*-RA on coactivator recruitment, SRC-1 peptide was titrated into the CAR−RXR(9-*cis*-RA) complex. This SRC-1 peptide also has a high affinity for RXR with a dissociation constant of 1.92 μM in the RAR−RXR heterodimer (*21*). As anticipated, the presence of the RXR agonist increases the apparent stoichiometry to two peptide molecules per CAR−RXR(9-*cis*-RA) heterodimer complex, and the data fit well to a noninteracting sites model indicating that both NR LBDs can bind the SRC-1 peptide independently (Figure 2). Since the two sites have similar K_d values for the peptide, their individual thermodynamic parameters cannot be determined and the results reflect contributions from both sites. While the overall enthalpic contribution is less favorable here than with either the apo or TCPOBOP-bound CAR−RXR complexes, the entropic contribution is nearly neutral (close to zero) in CAR−RXR(9-*cis*-RA) (Table 1). Unlike CAR which makes four H bonds with the coactivator, RXR forms only two H bonds with the coactivator peptide (*7*). K284 and E453 in RXR H bond with the residues at each end of the α-helical coactivator peptide (Figure S2B of the Supporting Information) (*7*). The remaining interactions between the peptide and RXR are apolar. Although the ΔH is less favorable in the RXR−SRC-1 interaction which is most likely due to the fact it has fewer H bonds than CAR−SRC-1, the comparable K_d can be explained by the compensating neutral $T\Delta S$ contribution.

Titrations were also performed in the presence of saturating concentrations of both TCPOBOP and 9-*cis*-RA (Figure 3). The isotherm from these titrations has a unique shape relative to those of the other titrations with CAR−RXR complexes (Figure 3A). As with the CAR−RXR(9-*cis*-RA) complex

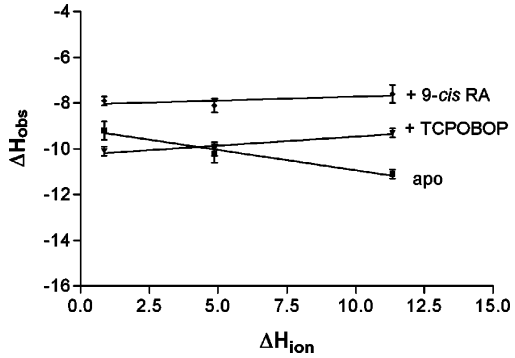

FIGURE 4: Enthalpy plotted as a function of the heat of ionization of phosphate, HEPES, and Tris-HCl buffers at pH 7.2 to determine the extent of binding-linked protonation.

Table 3: Amount of Net Proton Uptake by the CAR−RXR Complexes Resulting from SRC-1 Peptide Binding and the Intrinsic Enthalpy of the Reactions

complex	N_H	ΔH_{int} (kcal/mol)
CAR−RXR	−0.18	−9.1
CAR(TCPOBOP)−RXR	0.079	−10.2
CAR−RXR(9-*cis*-RA)	0.033	−8.0

above, the stoichiometry indicates two SRC-1 peptide molecules per CAR(TCPOBOP)−RXR(9-*cis*-RA) complex. Of the several models that were considered, the data fit best to a two-sets-of-sites model, where each site has its own binding characteristics (Figure 3B). Interestingly, in the presence of both ligands, one of the sites has a significantly increased affinity for the SRC-1 peptide relative to the affinity with either single ligand. A similar pattern in the binding of the coactivator to the two agonist-bound RAR−RXR heterodimers has been reported previously where a larger SRC-1 fragment with two intrinsic RIDs was used (*42*). The increase in the level of coactivator recruitment by the RAR−RXR heterodimer was proposed to be mediated by the unimolecular nature of the coactivator fragment as binding of one RID to one receptor brings the second RID into greater proximity to bind the partner NR. However, in this study, the titrations are performed with independent peptide molecules which are capable of binding each receptor separately. Therefore, the improved binding observed here must be mediated by conformational changes within the CAR−RXR heterodimer. This binding data may also explain the additive increase in the level of transcription measured in the presence of agonists for both CAR and RXR using DR-4-type response elements (*18*). However, the additive effect is not observed with other response elements.

Allosteric Contribution of RXR: Binding of SRC-1 to the CAR Monomer. RXR, the dimerization partner of CAR, has been shown to be critical for CAR activity. In two-hybrid assays, while only a very weak association is observed between uncomplexed CAR and SRC-1, the addition of exogenous RXR increases the level of recruitment of SRC-1 by CAR more than 3-fold (*14*). Indeed, RXR has been observed to allosterically regulate the activity of other heterodimeric partners, notably the retinoic acid receptor, RAR (*43*, *44*). To examine the role of RXR in CAR−SRC-1 interactions, we monitored global heat changes upon titration of the SRC-1 peptide into monomeric CAR. The binding isotherm suggests that the monomeric CAR−SRC-1 interaction (K_d = 21.3 μM) is substantially weaker than in the

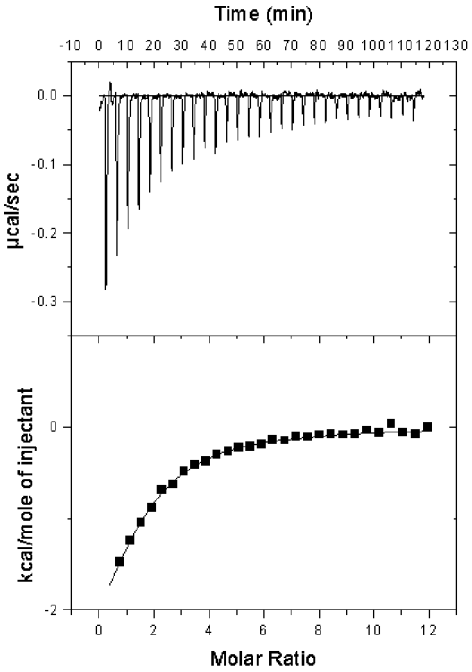

FIGURE 5: Binding of SRC-1 to monomeric CAR in the absence of ligand in 50 mM HEPES, 100 mM NaCl, and 1 mM TCEP (pH 7.2).

Table 4: Thermodynamic Parameters for Binding of SRC-1 Peptide to CAR[a]

	K_d (μM)	ΔH (kcal/mol)	$-T\Delta S$ (kcal/mol)	ΔG (kcal/mol)	N[b]
TCPOBOP	8.7 ± 0.8	−6.4 ± 0.5	−0.4	−6.8	0.96 ± 0.09
apo	21.3 ± 2.4	−5.8 ± 0.7	−0.6	−6.4	0.95 ± 0.10

[a] Determined at 25 °C and pH 7.2 in 50 mM HEPES, 0.1 M NaCl, and 1 mM TCEP. The reported values are the average of three experiments, and the errors are the standard deviation. [b] The apparent stoichiometry from the curve fitting data.

CAR−RXR heterodimer (K_d = 4.9 μM) (Figure 5 and Table 4). In the presence of saturating amounts of TCPOBOP, the CAR−SRC-1 binding improves (K_d = 8.7 μM), as in CAR-(TCPOBOP)−RXR (Table 4). This affinity for SRC-1 peptide in the presence of TCPOBOP is lower than with both apo CAR−RXR and CAR(TCPOBOP)−RXR in the same buffering system. Also, the improvement in SRC-1 binding from apo to TCPOBOP-bound monomeric CAR is primarily enthalpic, and the difference in ΔH is significantly large (>3 kcal/mol). This is in contrast to the effect of TCPOBOP on CAR−RXR, where entropic changes play a significant (unfavorable) role in SRC-1 peptide recruitment. Also in contrast to CAR−RXR, both the CAR−SRC-1 and CAR-(TCPOBOP)−SRC-1 complexes are associated with favorable changes in entropy. It is likely that in monomeric CAR, distal regions of the protein can undergo conformational changes to compensate for the loss of entropy that accompanies binding to SRC-1 peptide. In the more conformationally restricted CAR−RXR heterodimer, these regions may be restricted by RXR and the loss in entropy upon binding SRC-1 peptide is not adequately offset by conformational changes in CAR.

The overall lower K_d for binding of SRC-1 to monomeric CAR, compared to the CAR−RXR heterodimer, is largely a consequence of a significantly less favorable ΔH (Table 4). Thus, it is likely that the presence of RXR results in an

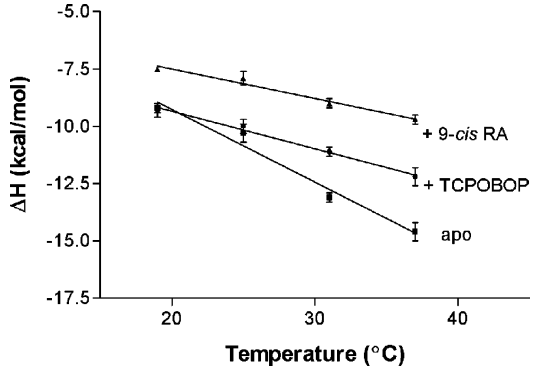

FIGURE 6: Observed enthalpy plotted as a function of temperature to determine ΔC_p for binding of SRC-1 peptide to apo CAR−RXR ($\Delta C_p = -320 \pm 30$ cal mol^{-1} K^{-1}), CAR(TCPOBOP)−RXR ($\Delta C_p = -160 \pm 20$ cal mol^{-1} K^{-1}), and CAR−RXR(9-*cis*-RA) ($\Delta C_p = -120 \pm 20$ cal mol^{-1} K^{-1}). Titrations contained 50 mM HEPES, 100 mM NaCl, and 1 mM TCEP, and the pH was adjusted to 7.2 at each temperature.

optimal geometric orientation of the CAR binding site for the SRC-1 peptide, resulting in a higher affinity between CAR and coactivator in the CAR−RXR heterodimer.

Structural Energetics and Change in Heat Capacity Associated with Coactivator Binding. The change in heat capacity (ΔC_p) in a protein−peptide interaction is analogous to that of protein unfolding and protein−ligand and protein−DNA interactions and depends primarily on the change in hydration due to the binding event (*45*); from ΔC_p, the change in solvent exposure of polar and nonpolar surfaces can be estimated (*33*, *46*, *47*). To determine ΔC_p for the binding of SRC-1 peptide to apo and liganded CAR−RXR heterodimers, titrations were performed at four different temperatures in HEPES and phosphate buffers. The heat capacity was determined from the slope of the linear regression fit when ΔH is plotted against the temperature at which the titration is performed (Figure 6).

A negative ΔC_p is observed in the formation all three CAR−RXR:coactivator complexes (Figure 6). There is very little change in affinity ($\delta\Delta G/\delta T \leq 0.1$ kcal K^{-1} mol^{-1}) between the SRC-1 peptide and the CAR−RXR heterodimer at the different temperatures. The effect of temperature on binding energetics is manifested in the change in the thermodynamic parameters, ΔH and $T\Delta S$. As the temperature is increased, there is a proportionate increase in the favorable ΔH, which is compensated by a decreasing favorable entropy (Figure S3 of the Supporting Information).

Using the published structure of the CAR(TCPOBOP)-(TIF2)−RXR(9-*cis*-RA)(TIF2) complex (PDB entry 1XLX) (*7*), we have estimated the ΔC_p upon binding of the coactivator to this complex. The two peptides that were used, the TIF2-derived peptide in the structure and the SRC-1 peptide in our titrations, are highly homologous and share the LXXLL motif; thus, the ΔASA calculated here should provide a very reasonable approximation of the apolar and polar exposed surface area. The calculated ΔASA values for binding of coactivator peptide to CAR(TCPOBOP) are as follows: $\Delta ASA_{apolar} = -765$ Å^2 and $\Delta ASA_{polar} = -394$ Å^2. Using eqs 3 and 4, the theoretical values for ΔC_p are −310 and −189 cal K^{-1} mol^{-1}, respectively. Our experimentally determined value for ΔC_p appears to agree with the theoretical treatment summarized in eq 4. The agreement of theoretical and experimental results suggests that the heat capacity change for this complex can be explained largely by the burial of solvent-exposed surface at the interface of CAR, and peptide and conformational changes distal to the SRC-1 binding site have a minimal effect on the binding energetics of the liganded complex. Binding of the SRC-1 peptide to apo CAR−RXR yields a significantly larger ΔC_p (−320 cal K^{-1} mol^{-1}). The absence of an apo CAR−RXR structure complexed with the coactivator peptide precludes a similar structural analysis and comparison. The 2-fold increase in ΔC_p when SRC-1 peptide binds the apo heterodimer compared to CAR(TCPOBOP)−RXR suggests significant differences in the conformations of the two complexes prior to coactivator binding. Since the surface area buried upon binding of SRC-1 peptide is likely to be similar in apo and CAR(TCPOBOP), the significantly larger ΔC_p for binding of SRC-1 apo CAR reiterates earlier observations that unliganded CAR is substantially more conformationally mobile than CAR(TCPOBOP). SRC-1 binding presumably induces changes in structure such that apolar surfaces distal to the coactivator binding site that were once exposed to solvent are buried upon binding the peptide. The theoretical values derived using eq 3 would require an alternate explanation. However, the entropy values described in Table 1 support the model described using eq 4.

The net energetic effects of structural changes within the free peptide and the bound, five-residue helical SRC-1 peptide should be similar in all titrations.

The calculated values for binding of coactivator peptide to RXR are as follows: $\Delta ASA_{apolar} = -814$ Å^2 and $\Delta ASA_{polar} = -467$ Å^2. These values lead to theoretical ΔC_p values of −318 and −195 cal K^{-1} mol^{-1} using eqs 7 and 8, respectively. The experimental value for ΔC_p is −120 cal K^{-1} mol^{-1} which is also closer to the value predicted by eq 8. However, the experimentally determined ΔC_p in this case reflects two events, binding of SRC-1 to CAR and RXR in the heterodimer. This lower experimental ΔC_p cannot accommodate the substantial changes in heat that accompany the relatively large conformational changes proposed by the ΔC_p observed in binding of SRC-1 peptide to apo CAR−RXR. This observation raises the interesting possibility that the RXR ligand can induce CAR into a conformation with a preformed coactivator binding site. In this scenario, coactivator recruitment of the CAR(TCPOBOP)−RXR(9-*cis*-RA) complex will not differ significantly from that of apo CAR−RXR(9-*cis*-RA). Cell-based transcriptional assays showing the effect of 9-*cis*-RA on CAR−RXR-mediated transcription activation in the absence of CAR agonist also support this model (*18*).

Conclusions. With respect to coactivator recruitment by the CAR−RXR heterodimer, our results imply that while the specific interactions in the CAR−SRC-1 assembly are similar, the enhanced transcriptional activity of CAR-(TCPOBOP) over apo CAR arises from a more effective recruitment of SRC-1 by a less conformationally ambiguous CAR(TCPOBOP). Additionally, the significance of RXR in coactivator recruitment is evident from the difference in the K_d and ΔH values in the monomeric CAR versus the CAR−RXR heterodimer.

The observed allosteric effect of the ligand of one receptor on the affinity at the coactivator binding site on the other NR in the heterodimer demonstrates that the increased level of transcription with both agonists is mediated by interactions

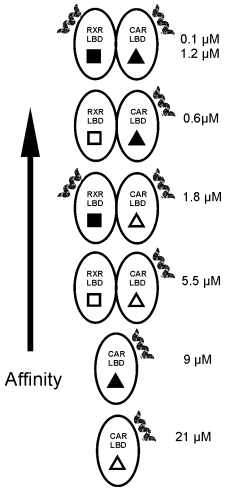

FIGURE 7: Effect of ligand and RXR on the affinity and stoichiometry of SRC-1 peptide. The short helix represents the bound peptide. The filled shapes indicate the presence of 9-*cis*-RA (■) and TCPOBOP (▲). The numbers to the right of the diagrams indicate the dissociation constant for the interaction(s).

between the two LBDs. Because of the complex nature of this data, additional experiments will be necessary to confirm this phenomenon. Titrations using mutants of RXR which are impaired in the ability to bind coactivator may be useful, but selection of mutations and data analysis can be complicated by the global effects of even a point mutation.

The ΔC_p data for the complexes also provide insight into the entropic contribution of binding of SRC-1 peptide to CAR−RXR. Two major components of the overall ΔS for a process are solvation and conformational entropy (*48*). Differences in solvation entropy will result from changes in the exposure of hydrophobic surfaces to solvent. The 2-fold difference in ΔC_p indicates that ΔS_{solv} would be more favorable in the unliganded heterodimer. Therefore, the more unfavorable ΔS_{total} observed for binding of SRC-1 peptide to apo CAR−RXR compared to CAR(TCPOBOP) must result from a more unfavorable ΔS_{conf}. This reflects a smaller difference in degrees of freedom between CAR(TCPOBOP)−RXR and CAR(TCPOBOP):SRC-1−RXR than differences in the NR−SRC-1 complexes in the absence of ligand. The agonist TCPOBOP reduces the ensemble of conformations of CAR−RXR by making specific interactions with CAR and thus reducing the flexibility of the CAR−RXR heterodimer.

The affinity and stoichiometry of the interactions of SRC-1 peptide with the various NR complexes are summarized in Figure 7. While these results demonstrate that the increasing affinity for coactivator and the increased level of transcription follow the same trend, a direct numerical correlation is not established (e.g., a 10-fold increase in peptide affinity leads to an only 3-fold increase in the level of transcription). This discrepancy is probably due to the other events that occur after SRC-1 recruitment and prior to initiation of transcription.

This study is likely to have general implications on the underlying mechanics of SRC-1 recruitment and RXR-mediated allosterism and may well be a common feature within the NR superfamily. The sequence of events in ligand binding, coactivator recruitment, and the underlying interactions between heterodimeric partners, ligand−receptor and receptor−coactivator, are remarkably conserved. Further studies with larger SRC-1 fragments and full-length NRs in the presence of specific RE-derived DNA fragments may reveal the mechanism of coactivator recruitment in even greater detail.

ACKNOWLEDGMENT

We thank Drs. Barry Forman, Elizabeth Howell, and Engin Serpersu for critical reading of the manuscript and helpful suggestions. We also thank Mr. Sumit Patel for protein preparation.

SUPPORTING INFORMATION AVAILABLE

Chromatograms showing oligomeric states of CAR−RXR and monomeric CAR after ITC titrations (Figure S1), the hydrogen bonds formed between the peptide and CAR−RXR (Figure S2), and graphs of ΔG and $-T\Delta S$ as a function of temperature (Figure S3). This material is available free of charge via the Internet at http://pubs.acs.org.

REFERENCES

1. Torchia, J., Glass, C., and Rosenfeld, M. G. (1998) Co-activators and co-repressors in the integration of transcriptional responses, *Curr. Opin. Cell Biol. 10*, 373−83.
2. Onate, S. A., Tsai, S. Y., Tsai, M. J., and O'Malley, B. W. (1995) Sequence and characterization of a coactivator for the steroid hormone receptor superfamily, *Science 270*, 1354−7.
3. Nolte, R. T., Wisely, G. B., Westin, S., Cobb, J. E., Lambert, M. H., Kurokawa, R., Rosenfeld, M. G., Willson, T. M., Glass, C. K., and Milburn, M. V. (1998) Ligand binding and co-activator assembly of the peroxisome proliferator-activated receptor-gamma, *Nature 395*, 137−43.
4. Kalkhoven, E., Valentine, J. E., Heery, D. M., and Parker, M. G. (1998) Isoforms of steroid receptor co-activator 1 differ in their ability to potentiate transcription by the oestrogen receptor, *EMBO J. 17*, 232−43.
5. McInerney, E. M., Rose, D. W., Flynn, S. E., Westin, S., Mullen, T. M., Krones, A., Inostroza, J., Torchia, J., Nolte, R. T., Assa-Munt, N., Milburn, M. V., Glass, C. K., and Rosenfeld, M. G. (1998) Determinants of coactivator LXXLL motif specificity in nuclear receptor transcriptional activation, *Genes Dev. 12*, 3357−68.
6. Watkins, R. E., Wisely, G. B., Moore, L. B., Collins, J. L., Lambert, M. H., Williams, S. P., Willson, T. M., Kliewer, S. A., and Redinbo, M. R. (2001) The human nuclear xenobiotic receptor PXR: Structural determinants of directed promiscuity, *Science 292*, 2329−33.
7. Suino, K., Peng, L., Reynolds, R., Li, Y., Cha, J. Y., Repa, J. J., Kliewer, S. A., and Xu, H. E. (2004) The nuclear xenobiotic receptor CAR: Structural determinants of constitutive activation and heterodimerization, *Mol. Cell 16*, 893−905.
8. Shiau, A. K., Barstad, D., Loria, P. M., Cheng, L., Kushner, P. J., Agard, D. A., and Greene, G. L. (1998) The structural basis of estrogen receptor/coactivator recognition and the antagonism of this interaction by tamoxifen, *Cell 95*, 927−37.
9. Darimont, B. D., Wagner, R. L., Apriletti, J. W., Stallcup, M. R., Kushner, P. J., Baxter, J. D., Fletterick, R. J., and Yamamoto, K. R. (1998) Structure and specificity of nuclear receptor-coactivator interactions, *Genes Dev. 12*, 3343−56.
10. Moras, D., and Gronemeyer, H. (1998) The nuclear receptor ligand-binding domain: Structure and function, *Curr. Opin. Cell Biol. 10*, 384−91.
11. Wei, P., Zhang, J., Egan-Hafley, M., Liang, S., and Moore, D. D. (2000) The nuclear receptor CAR mediates specific xenobiotic induction of drug metabolism, *Nature 407*, 920−3.
12. Zhang, J., Huang, W., Chua, S. S., Wei, P., and Moore, D. D. (2002) Modulation of acetaminophen-induced hepatotoxicity by the xenobiotic receptor CAR, *Science 298*, 422−4.
13. Huang, W., Zhang, J., and Moore, D. D. (2004) A traditional herbal medicine enhances bilirubin clearance by activating the nuclear receptor CAR, *J. Clin. Invest. 113*, 137−43.

14. Dussault, I., Lin, M., Hollister, K., Fan, M., Termini, J., Sherman, M. A., and Forman, B. M. (2002) A structural model of the constitutive androstane receptor defines novel interactions that mediate ligand-independent activity, *Mol. Cell. Biol. 22*, 5270−80.
15. Forman, B. M., Tzameli, I., Choi, H. S., Chen, J., Simha, D., Seol, W., Evans, R. M., and Moore, D. D. (1998) Androstane metabolites bind to and deactivate the nuclear receptor CAR-β, *Nature 395*, 612−5.
16. Tzameli, I., Pissios, P., Schuetz, E. G., and Moore, D. D. (2000) The xenobiotic compound 1,4-bis[2-(3,5-dichloropyridyloxy)]-benzene is an agonist ligand for the nuclear receptor CAR, *Mol. Cell. Biol. 20*, 2951−8.
17. Maglich, J. M., Parks, D. J., Moore, L. B., Collins, J. L., Goodwin, B., Billin, A. N., Stoltz, C. A., Kliewer, S. A., Lambert, M. H., Willson, T. M., and Moore, J. T. (2003) Identification of a novel human constitutive androstane receptor (CAR) agonist and its use in the identification of CAR target genes, *J. Biol. Chem. 278*, 17277−83.
18. Tzameli, I., Chua, S. S., Cheskis, B., and Moore, D. D. (2003) Complex effects of rexinoids on ligand dependent activation or inhibition of the xenobiotic receptor, CAR, *Nucl. Recept. 1*, 2−9.
19. Shan, L., Vincent, J., Brunzelle, J. S., Dussault, I., Lin, M., Ianculescu, I., Sherman, M. A., Forman, B. M., and Fernandez, E. J. (2004) Structure of the murine constitutive androstane receptor complexed to androstenol: A molecular basis for inverse agonism, *Mol. Cell 16*, 907−17.
20. Xu, R. X., Lambert, M. H., Wisely, B. B., Warren, E. N., Weinert, E. E., Waitt, G. M., Williams, J. D., Collins, J. L., Moore, L. B., Willson, T. M., and Moore, J. T. (2004) A structural basis for constitutive activity in the human CAR/RXRα heterodimer, *Mol. Cell 16*, 919−28.
21. Pogenberg, V., Guichou, J. F., Vivat-Hannah, V., Kammerer, S., Perez, E., Germain, P., de Lera, A. R., Gronemeyer, H., Royer, C. A., and Bourguet, W. (2005) Characterization of the interaction between retinoic acid receptor/retinoid X receptor (RAR/RXR) heterodimers and transcriptional coactivators through structural and fluorescence anisotropy studies, *J. Biol. Chem. 280*, 1625−33.
22. Ye, H., and Wu, H. (2000) Thermodynamic characterization of the interaction between TRAF2 and tumor necrosis factor receptor peptides by isothermal titration calorimetry, *Proc. Natl. Acad. Sci. U.S.A. 97*, 8961−6.
23. Goto, N. K., Zor, T., Martinez-Yamout, M., Dyson, H. J., and Wright, P. E. (2002) Cooperativity in transcription factor binding to the coactivator CREB-binding protein (CBP). The mixed lineage leukemia protein (MLL) activation domain binds to an allosteric site on the KIX domain, *J. Biol. Chem. 277*, 43168−74.
24. Adhikari, A., and Sprang, S. R. (2003) Thermodynamic characterization of the binding of activator of G protein signaling 3 (AGS3) and peptides derived from AGS3 with Gαi1, *J. Biol. Chem. 278*, 51825−32.
25. Murphy, K. P., Freire, E., and Paterson, Y. (1995) Configurational effects in antibody-antigen interactions studied by microcalorimetry, *Proteins 21*, 83−90.
26. Raman, C. S., Allen, M. J., and Nall, B. T. (1995) Enthalpy of antibody−cytochrome c binding, *Biochemistry 34*, 5831−8.
27. Baker, B. M., and Murphy, K. P. (1997) Dissecting the energetics of a protein-protein interaction: The binding of ovomucoid third domain to elastase, *J. Mol. Biol. 268*, 557−69.
28. Wright, E., and Serpersu, E. H. (2005) Enzyme-substrate interactions with an antibiotic resistance enzyme: Aminoglycoside nucleotidyltransferase(2″)-Ia characterized by kinetic and thermodynamic methods, *Biochemistry 44*, 11581−91.
29. He, B., and Wilson, E. M. (2003) Electrostatic modulation in steroid receptor recruitment of LXXLL and FXXLF motifs, *Mol. Cell. Biol. 23*, 2135−50.
30. Wiseman, T., Williston, S., Brandts, J. F., and Lin, L. N. (1989) Rapid measurement of binding constants and heats of binding using a new titration calorimeter, *Anal. Biochem. 179*, 131−7.
31. Goldberg, R. N., Kishore, N., and Lennen, R. M. (2002) Thermodynamic Quantities for the Ionization Reactions of Buffers, *J. Phys. Chem. Ref. Data 31*, 231−370.
32. Fukada, H., and Takahashi, K. (1998) Enthalpy and heat capacity changes for the proton dissociation of various buffer components in 0.1 M potassium chloride, *Proteins 33*, 159−66.
33. Murphy, K. P., and Freire, E. (1992) Thermodynamics of structural stability and cooperative folding behavior in proteins, *Adv. Protein Chem. 43*, 313−61.
34. Spolar, R. S., Livingstone, J. R., and Record, M. T., Jr. (1992) Use of liquid hydrocarbon and amide transfer data to estimate contributions to thermodynamic functions of protein folding from the removal of nonpolar and polar surface from water, *Biochemistry 31*, 3947−55.
35. Baker, B. M., and Murphy, K. P. (1996) Evaluation of linked protonation effects in protein binding reactions using isothermal titration calorimetry, *Biophys. J. 71*, 2049−55.
36. Gomez, J., and Freire, E. (1995) Thermodynamic mapping of the inhibitor site of the aspartic protease endothiapepsin, *J. Mol. Biol. 252*, 337−50.
37. Choi, H. S., Chung, M., Tzameli, I., Simha, D., Lee, Y. K., Seol, W., and Moore, D. D. (1997) Differential transactivation by two isoforms of the orphan nuclear hormone receptor CAR, *J. Biol. Chem. 272*, 23565−71.
38. Johnson, B. A., Wilson, E. M., Li, Y., Moller, D. E., Smith, R. G., and Zhou, G. (2000) Ligand-induced stabilization of PPARγ monitored by NMR spectroscopy: Implications for nuclear receptor activation, *J. Mol. Biol. 298*, 187−94.
39. Moore, L. B., Parks, D. J., Jones, S. A., Bledsoe, R. K., Consler, T. G., Stimmel, J. B., Goodwin, B., Liddle, C., Blanchard, S. G., Willson, T. M., Collins, J. L., and Kliewer, S. A. (2000) Orphan nuclear receptors constitutive androstane receptor and pregnane X receptor share xenobiotic and steroid ligands, *J. Biol. Chem. 275*, 15122−7.
40. Heyman, R. A., Mangelsdorf, D. J., Dyck, J. A., Stein, R. B., Eichele, G., Evans, R. M., and Thaller, C. (1992) 9-*cis*-Retinoic acid is a high affinity ligand for the retinoid X receptor, *Cell 68*, 397−406.
41. Shulman, A. I., Larson, C., Mangelsdorf, D. J., and Ranganathan, R. (2004) Structural determinants of allosteric ligand activation in RXR heterodimers, *Cell 116*, 417−29.
42. Germain, P., Iyer, J., Zechel, C., and Gronemeyer, H. (2002) Co-regulator recruitment and the mechanism of retinoic acid receptor synergy, *Nature 415*, 187−92.
43. Kurokawa, R., DiRenzo, J., Boehm, M., Sugarman, J., Gloss, B., Rosenfeld, M. G., Heyman, R. A., and Glass, C. K. (1994) Regulation of retinoid signalling by receptor polarity and allosteric control of ligand binding, *Nature 371*, 528−31.
44. Forman, B. M., Umesono, K., Chen, J., and Evans, R. M. (1995) Unique response pathways are established by allosteric interactions among nuclear hormone receptors, *Cell 81*, 541−50.
45. Sturtevant, J. M. (1977) Heat capacity and entropy changes in processes involving proteins, *Proc. Natl. Acad. Sci. U.S.A. 74*, 2236−40.
46. Spolar, R. S., and Record, M. T., Jr. (1994) Coupling of local folding to site-specific binding of proteins to DNA, *Science 263*, 777−84.
47. Myers, J. K., Pace, C. N., and Scholtz, J. M. (1995) Denaturant m values and heat capacity changes: Relation to changes in accessible surface areas of protein unfolding, *Protein Sci. 4*, 2138−48; (1996) *5* (5), 981 (erratum).
48. Lee, K. H., Xie, D., Freire, E., and Amzel, L. M. (1994) Estimation of changes in side chain configurational entropy in binding and folding: General methods and application to helix formation, *Proteins 20*, 68−84.

BI061627I